COBEM 99
XV Congresso Brasileiro de Engenharia Mecânica
15th Brazilian Congress of Mechanical Engineering
22 - 26 de Novembro de 1999 / November 22 - 26, 1999 Águas de Lindóia, São Paulo,

ON THE CHARACTERISATION OF AIR/FUEL MIXTURE DISTRIBUTION THROUGH C_2/CH CHEMILUMINESCENCE RATIO IN A LPP COMBUSTOR

A. Caldeira-Pires
P. Anacleto
Instituto Superior Técnico
Av. Rovisco Pais, 1049-001 - Lisbon - Portugal
email: armando@dem.ist.utl.pt
F. S. Costa
Instituto Nacional de Pesquisas Espaciais
Rod. Pres. Dutra, km 40, 12630-000 Cachoeira Paulista, SP, Brasil
P. T. Lacava
Instituto Tecnológico da Aeronáutica
Centro Técnico Aeroespacial, 12228-900 São José dos Campos, SP,
J. A. Carvalho-Jr
Universidade Estadual Paulista
Campus de Guaratinguetá, Guaratinguetá, SP, Brasil

Abstract. This paper discusses the utilisation of C_2/CH chemiluminescence ratio as a diagnostic technique to assess mixture non-homogeneities within liquid fuel lean premixed flames burning inside a laboratory scale model of a LPP combustion chamber. C_2 and CH monochromic projections are tomographically reconstructed to obtain their three-dimensional distribution, which allows the spatial correlation of C_2 and CH fields at several gaseous and liquid fuel equivalence ratio/vanes angle combinations. The influence of vanes angle depicts that non-swirling flame is bluff-body stabilised, and as the swirl increases, a new recirculation zone is induced, bending the flame and concentrating the reaction zone within the first section of the combustion chamber. The relationship between C_2/CH ratio and equivalence ratio for propane flames shows that intensity ratio increases simultaneously with equivalence ratio, as well as the difference between the maximum and minimum values of C_2/CH ratio, probably due to incomplete mixing. The utilisation of local C_2/CH ratio is therefore related to equivalence ratio and can assess useful information on the quality of the mixing process. The present results provide new information on the characterisation of mixture homogeneity of lean premixing flames within practical combustion chamber geometry. The results reinforce the qualitative compromise between light intensity and mixing conditions.

Keywords: *Gas Turbine; C_2 and CH Chemiluminescence; Tomographic Reconstruction*

1 INTRODUCTION

Exhaust emissions from gas turbine engines have been a relevant issue for researchers and engineers since the 60s because of their chemical compounds, namely unburned hydrocarbons and nitric and carbon oxides, which can directly or indirectly harm environment and human health. The demands for preservation of the ozone layer have imposed new limitations in terms of reduction of NO_x emissions of gas turbines conventional technology used by aeronautical industry. This approach has motivated the development of new technologies for the design of future combustion chamber for these engines.

In this context, considerable progress have been made in the last 20 years at North American industry (e.g. Bahr, 1995), as well as at European level (e.g. Joos and Pellischeck, 1995), that facilitates to identify new concepts with larger success probability in the reduction of the environmental impact of the airships. In particular, it is expected that the premixing pre-vaporisation technology (LPP - lean premixed pre-vaporised) allows for in the next decades reductions of about 90% in the levels of NO_x, relatively to the current technology.

This technology consists in pre-vaporising and premixing the fuel with hot air below the stoichiometric conditions in a first stage of the combustor, and then burning this mixture at lean conditions and low temperatures in a second stage, the combustion chamber itself. This approach avoids the occurrence of high temperatures responsible for the production of thermal NO_x. A major issue on this technology has been the air/fuel mixture inhomogeneity, in which poor mixture homogeneity may cause incomplete combustion and affects directly the efficiency of the combustion process. Understanding the spatial air/fuel mixture distribution may help the design of fuel-discharge system, as well as combustion chamber, which in turn may improve the combustion process and reduce exhaust emissions.

This work aims at deepening the knowledge of turbulent mixing phenomena occurring in the reaction zone in gas turbines combustion chambers, to facilitate an improved control of the combustion processes in the future engines with practical application. This study will discuss the development of an experimental method of characterisation of mixture inhomogeneities, based on the acquisition of the radiation emitted by CH and C_2 free radicals, inside a laboratory scale model of a LPP combustion chamber.

The monochrome image projected by these chemical species is acquired at characteristic wavelengths, respectively 431nm and 514nm. Tomographic reconstruction techniques are applied to each projection to obtain the three-dimensional distribution of these chemical species emissions, which will allow spatial correlation of C_2 and CH fields. The intensity variation of CH and C_2 with mixture strengths has been reported in the literature since Gaydon (1957). In general, C_2 bands are strongest with very rich mixtures, while CH dominates in the lean and less fuel rich conditions. As suggested by Chou and Petterson (1995), taking the intensity ratio of C_2 and CH can eliminate the effects of combustion pressure and temperature.

This article divides in four sections. The description of the experimental installation and diagnostics techniques is presented in the next section. The results are discussed in the third section, and the main conclusions are then summarised.

2 EXPERIMENTAL CONDITIONS

The combustor geometry. Figure 1 shows the schematic diagram of the physical model used in this study, which encompassed a premixing prevaporising chamber and the combustion chamber, itself. A bluff-body is positioned at the entrance of the combustion chamber to stabilise the flame. Anacleto (1993) and Anacleto and Heitor (1997) provide a detailed description of this installation rig.

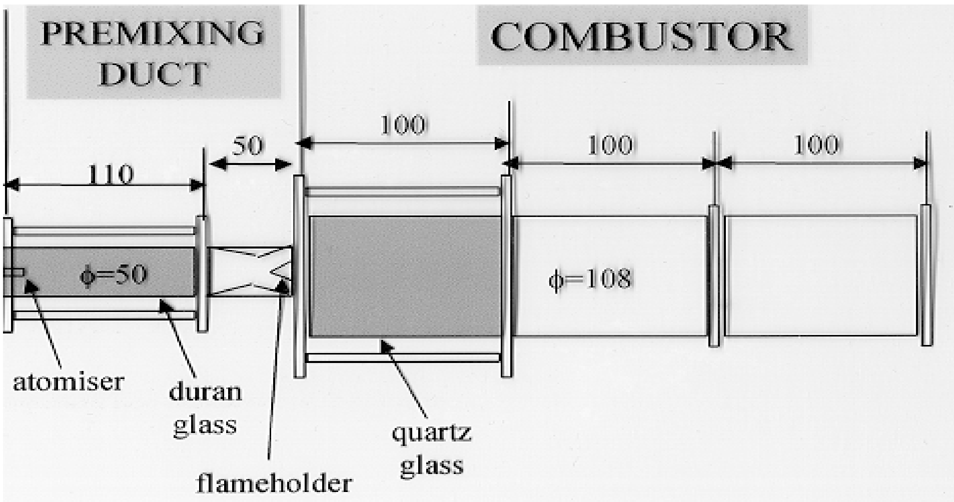

Figure 1 Schematic Diagram of the Combustor Model (lengths in mm)

The flow conditions. The measurements were performed for propane at equivalence ratio, Φ, conditions ranging from 0.6 to 1.5, and angle of swirl vanes, ω, from 0º to 60º. Within these conditions, Reynolds number varied between 35000 and 38000. Experiments were also performed with liquid fuel AVGAS, at Φ=0.5 and 0.8, and the same swirl angles range.

Image acquisition system. A CCIR camera was placed perpendicular to the quartz section of the combustor, obtaining radial views of the flame. The video output signals were connected to a RGBA frame grabber, and used for the acquisition of two independent monochromatic video signals. A commercial 50mm lens (f = 1.4) allowed a cone collection of light of 20^o, minimising the distortion due to wide-angle imaging.

Visible interference filters (centred at 432 and 515nm, with transmittance of 0.55 and 0.66 at 10% of maximum transmissivity) were used for acquisition of monochromatic flame images. A dedicated software library was used in order to control the frame grabber. Tomographic reconstruction software was purpose built, performing images ratio calculation as well, as described by Correia et al. (1998) and Costa et al. (1998).

The flame images acquisition procedure consisted on obtaining time-averaged images for the two wavelengths, for a single projection, as the average flame characteristics are axi-symmetric.

Figure 2 shows the tomographic reconstruction process applied on a propane C_2 flame image, at Φ=0.6 and ω = 40^o depicting reaction and recirculation zones within the combustion chamber.

The influence of exposition time and diaphragm aperture on the shape and intensity of acquired images was assessed, showing that the area comprised by the reaction zone, characterised by C_2/CH ratio images, is depicted at the same position as the aperture ranges from f=1.4 to 2.8. As well, the shape of this region is not altered with the exposition time, from t=1/250 to 1/500s, although it can be detected small differences on the grey scale intensity at lower exposition time.

Influence of equivalence ratio on C_2 and CH concentration. Figure 3 presents the calculated evolution of maximum value of the mole fraction for C_2 and CH radicals, as well as C_2/CH ratio as a function of equivalence ratio for propane combustion with air. The calculations were made for initial value problem using the computational code CHEMKIN II (Kee et al, 1992). The pressure was kept constant at 1bar . For all simulations the gas initial temperature was 1000 K, to provide enough energy for ignition. The kinetic mechanism employed was taken from detailed reaction mechanism for small hydrocarbons combustion proposed by Konnov (1998), and involves 122 chemical species with 1027 elementary reactions.

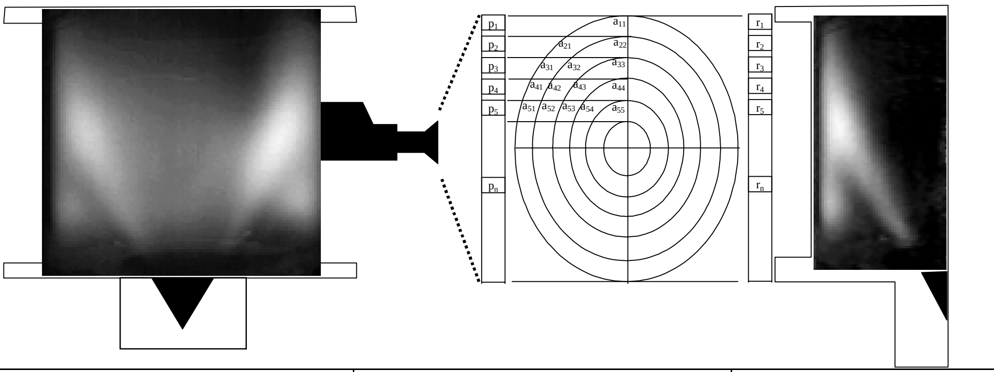

C_2 Mean Projection	Tomographic Reconstruction Process	C_2 Reconstructed Image

Figure 2 Mean Projection and Reconstructed Image of C_2 emission from Propane flame; Φ=0.6; $\omega = 40^o$ (the bluff body drawing locates the flame inside the combustion chamber)

Maximum mole fraction value occurred simultaneously for both radicals. C_2 and CH radicals peak concentration increase until a maximum value Φ = 1,4, decreasing as the equivalence ratio increases up to Φ = 2. That decrease probably took place due to competition among intermediary radicals in rich conditions. C_2/CH ratio evaluation shows that in spite of the growth of both radicals, the relative growth of C_2 is larger than CH, from Φ = 0.6 to Φ = 1.4. Above Φ = 1.4, C_2 concentration decreased faster than CH. Therefore, for well-mixed conditions of lean combustion, a low value of C_2/CH ratio is expected.

3 RESULTS

CH and C_2 emission at propane premixed flames. Monochromatic intensities of CH and C_2 were measured at equivalence ratios ranging from Φ = 0.6 to 1.5 and vanes angle from $\omega = 0^o$ to 60^o.

Figure 4 presents CH reconstructed images, displaying the influence of swirl on the length and the position of propane premixed flame (C_2 images show similar trends). Initially, the non-swirl flame was stabilised by the bluff-body disk, occupying the whole quartz chamber and part of the steel chamber, although the highest intensity position was located at the end of the quartz section. As the swirl increases, a new recirculation zone was created, bending the flame and concentrating the reaction zone within the quartz section. Maximum intensity value at both wavelengths was not altered due to the vanes angle. However, CH intensity signal was stronger than C_2 within the range of vanes angle analysed.

Figure 5 shows the evolution of CH reconstructed images with equivalence ratio for $\omega = 40^o$. The overall results depict the dominance of CH emission on C_2 emission up to Φ =1.2. Between Φ =1.3 to 1.5 CH and C_2 emissions present similar intensities values. It was not detected any influence of the equivalence ratio on the flame shape among images of the same wavelength. Small differences between the shape of CH and C_2 images can be explained due to the emission relaxation time of each free radical, namely CH persists up to 10^{-5} s and C_2 10^{-7} s, as reported by Mokaddem et al (1994) and Nguyen and Paul (1996). The higher emission relaxation time of CH allows that it remain emitting while is transported to the recirculation zone, therefore presenting higher emitting areas than C_2, as suggested by Fernandes (1998).

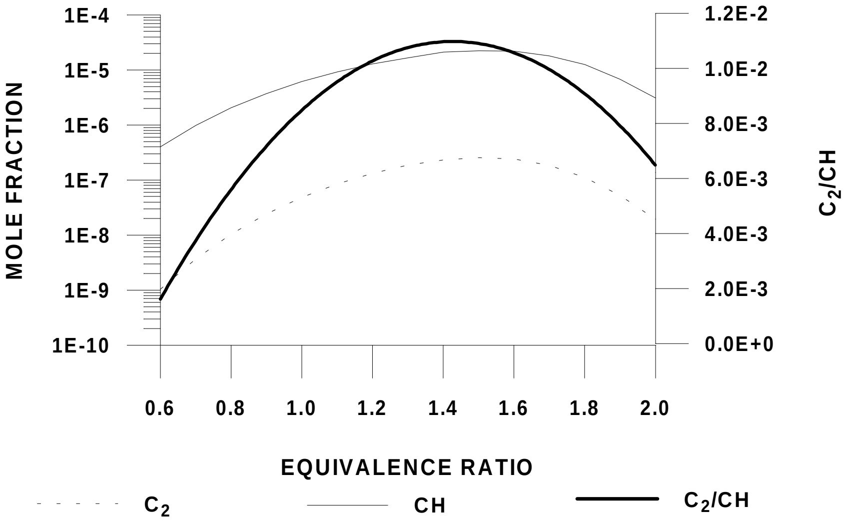

Figure 3 Time Evolution of C_2 and CH mole fraction and C_2/CH ratio with Equivalence Ratio, **Φ**; simulation of a batch reaction with CHEMKIN; Propane.

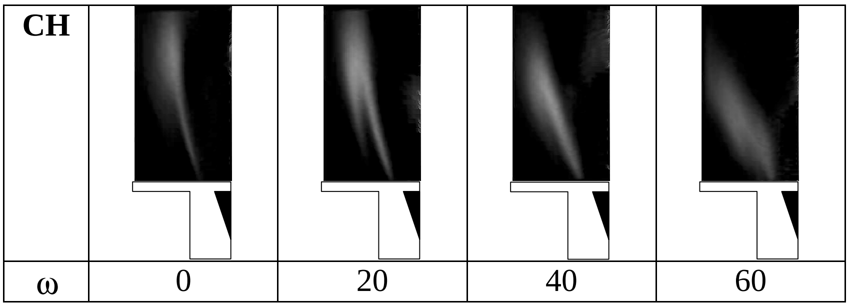

Figure 4 Influence of Vanes angle, ω, on CH emissions; Reconstructed images; Propane; **Φ** = 1 (the bluff body drawing locates the flame inside the combustion chamber)

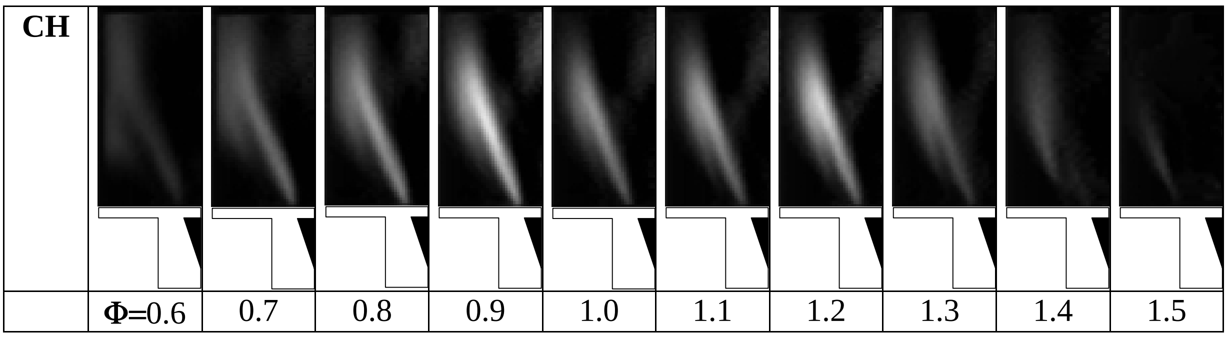

Figure 5 Influence of Equivalence Ratio, **Φ**, on C_2 and CH emissions; Reconstructed images; Propane; ω = 40°.

C_2/CH ratio characteristics. The intensity variation of CH and C_2 radicals strongly depends on the mixture strength, as stated by Gaydon (1957). From a general point of view, C_2 bands are strongest with very rich mixtures and CH bands are strongest at mixtures below stoichiometry.

Figure 6 displays the evolution of maximum intensity values with equivalence ratio, depicting the relative importance between the CH and C_2 intensities. In the images analysed, while CH emission dominates at lean flames, C_2 radical controls emission within the rich region, which corroborates measurements formerly reported by Gaydon (1957) and more recently by Yamazaki et al (1990).

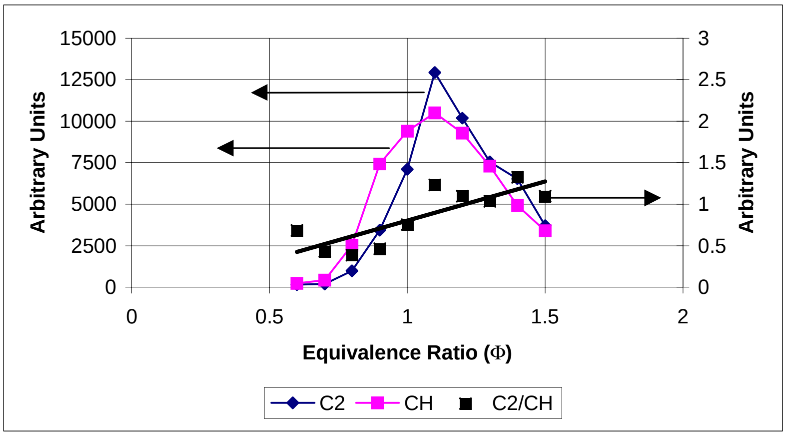

Figure 6 Evolution of maximum value of light intensity of C_2 and CH reconstructed images with Equivalence Ratio, Φ; Propane; $\omega = 40^o$.

Comparison between Figure 6 and Figure 3 displays that both cases of evolution of the C_2/CH mole fraction ratio present a continuous increasing of CH over C_2 through the range of equivalence ratio analysed.

Due to the difference between relaxation emission time of the two free radicals, it must be determined to each pair of images the region of the C_2 image before the pixel by pixel calculation of the intensities ratio. This region is used to build a high-pass filter that is applied to CH image in order to limit its extension to the same location of C_2 image. The rest of the pixels are set to zero, precluding the relationship between pixels with and without relevant information and excluding the bluff-body recirculation noisily region. This procedure is applied every time C_2/CH ratio is analysed.

Moreover, this operation also prevents that the flame emission due to CO_2 and CO masks the free radicals emissions. CO_2 and CO show a strong continuous spectrum from 300 to 550nm, which overlaps the CH and C_2 band used in this research. However, since this CO_2 and CO formation reactions occurred after the flame front passed through, the utilisation of the C_2 location as a filter avoids the incorporation of non-relevant information to this process.

Figure 7 shows the influence of equivalence ratio on C_2/CH intensity ratio. The images shown in this figure do not present significant variation in the flame shape and location between $\Phi = 0.7$ and 1.3. At $\Phi = 0.6$, complete mixing and low intensities of both C_2 and CH difficult the exact characterisation of C_2/CH intensity ratio image. Otherwise, at $\Phi = 1.4$ and 1.5, incomplete mixing causes a deformation of the C_2 image that is used to limit the region to be analysed within the combustion chamber, and depicted a flame front shape different from those displayed by the other equivalence ratio conditions.

Otherwise, the evolution of image histograms with equivalence ratio shown in Figure 8 depicts that intensity ratio, in 8bits grey scale, increases as equivalence ratio increases and that variation of intensity ratio (difference between maximum and minimum values of intensity ratio) at a given equivalence ratio is relatively small. For increasing equivalence ratio, the difference between the maximum and minimum values of C_2/CH ratio increases, probably caused by incomplete mixing. For instance, as the amount of fuel delivered to air stream increases, a longer mixing length may be needed to generate a homogeneous mixture. This phenomenon introduces some uncertainties in applying this diagnostic method, since variations of intensity ratios became more prominent at extremely rich mixtures due to incomplete mixing.

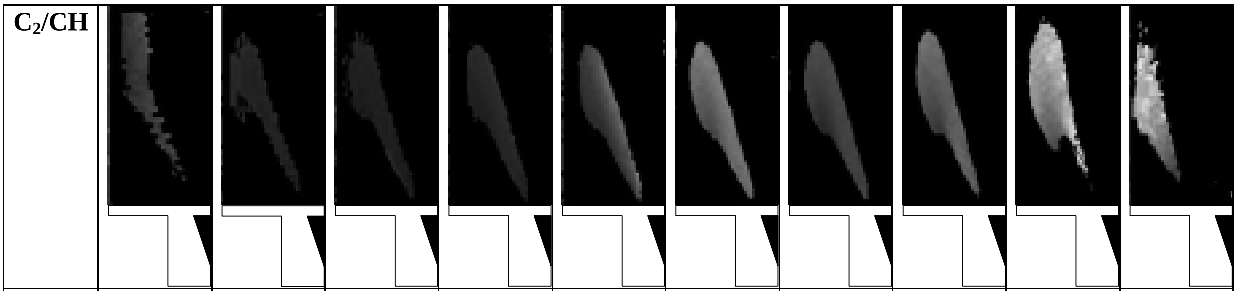

Φ	0.6	0.7	0.8	0.9	1.0	1.1	1.2	1.3	1.4	1.5

Figure 7 Influence of Equivalence Ratio, **Φ**, on C_2/CH ratio images; Propane; $\omega = 40^o$.

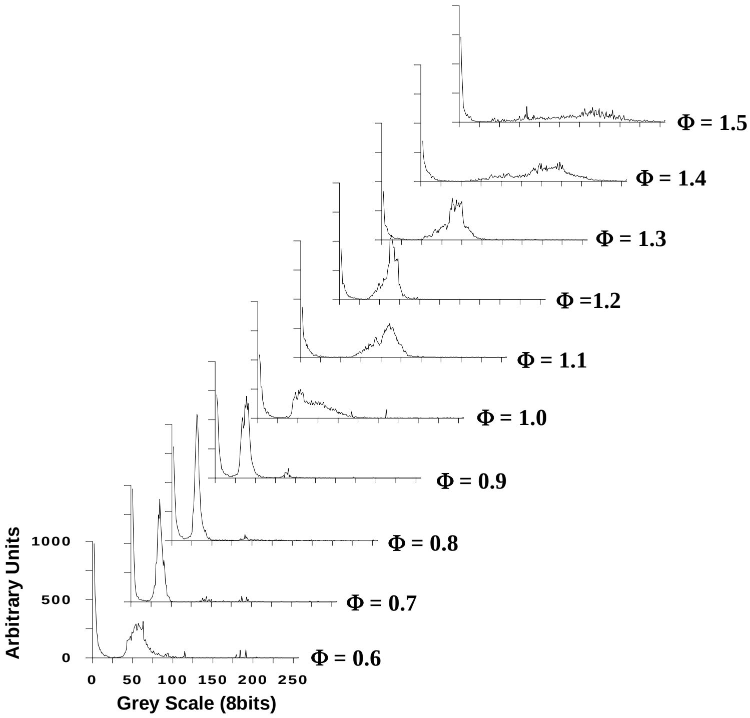

Figure 8 Evolution of histogram of light intensity of C_2/CH ratio with Equivalence Ratio, **Φ**; Propane; $\omega = 40^o$.

Figure 9 shows the evolution of C_2/CH ratio images with vanes angle, highlighting the influence of the rotational movement on the flame front concentration near the outlet of mixed reactants. As the swirl increases a new recirculation region is induced and the combustion reactions concentrate into a smaller zone of the combustor volume. Nevertheless, the histogram mean value does not varies as vanes angle ranges from 0^o to 40^o, since the length of premixing duct is enough to promote a good mix for gases, independent of vanes angle.

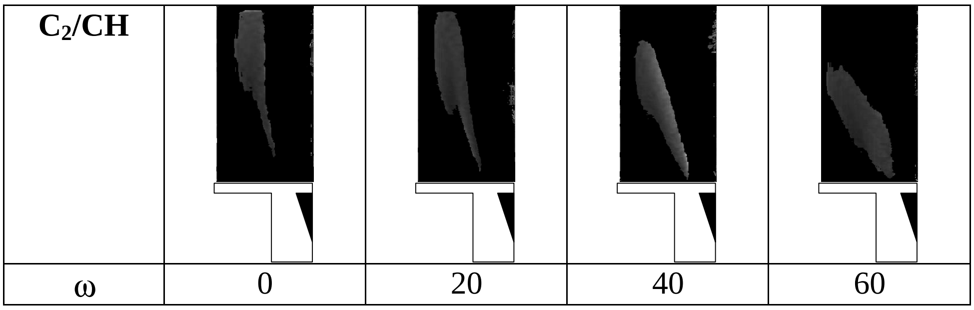

Figure 9 Influence of Vanes angle, ω, on C_2/CH images; Reconstructed images; Propane; **Φ** = 1 (bluff body drawing locates the flame inside the combustion chamber)

Aeronautic liquid fuel results - fuel/air mixture distribution analysis. Aeronautic liquid fuel combustion is discussed in this section, attempting to establish a correlation with propane flame conditions. Figure 10 shows C_2/CH ratio results, encompassing measurements performed at two fuel mass flow rate, namely Φ = 0.5 and 0.8, and four vanes angle conditions, ω = 0, 20, 35 and 55^o.

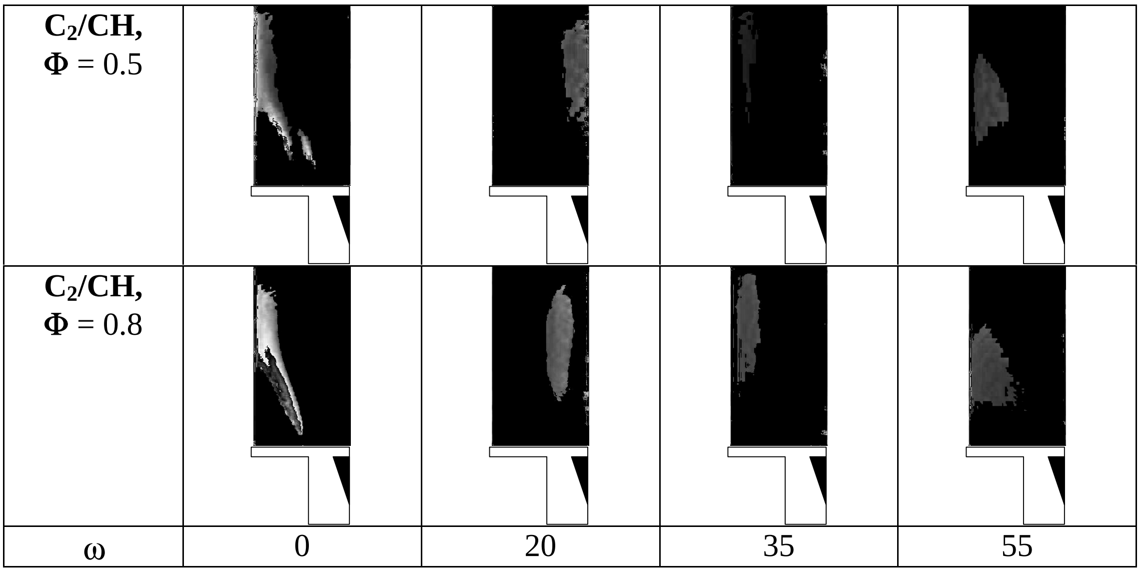

Figure 10 Influence of Vanes angle, ω, and Equivalence Ratio, Φ, on C_2/CH ratio images; Propane.

Both equivalence ratio conditions show similar behaviour regarding the swirl level. Firstly in the non-rotational flow, the smaller path length within the pre-camera does not allow that fuel vaporisation and air/fuel mixing processes to complete. This is identified by the saturated images at ω = 0, where highly luminous flames take place due to non-vaporised fuel droplets impinging the quartz wall and burning within the combustion chamber. These flames are highly unstable.

As the swirling increases, the air/fuel mixture is conveyed to the bluff-body recirculation zone, where the combustion occurs. Subsequent increasing of the swirling first centrifuges the reactant mixture toward the quartz cylinder and then concentrates the flame into the recirculation zone, following the same pattern presented by propane flows.

The differences between the two conditions are depicted only by the light intensity level, whereas the smaller Φ displays lower values of the grey scale. As a general analysis, the four swirling flames present similar histograms, all of them spreading the grey level distribution over a wider range than those measured with propane, probably due to lower efficiency in the mixing process.

4 CONCLUSIONS

This study characterised the combustion phenomena within a premixing prevaporisation combustion chamber (LPP - lean premixed prevaporised). The air/fuel mixture inhomogeneity, in which poor mixture homogeneity may cause incomplete combustion, is assessed through the intensity variation between CH/C_2 emissions ratio with mixture strengths.

Gaseous and liquid fuels were used to assess air/fuel mixture distribution at the combustion chamber, namely propane and jet fuel AVGAS. The measurements were performed varying equivalence ratio, ranging from 0.6 to 1.5 for propane combustion, and 0.5 and 0.8 for liquid combustion, and vanes angle, ranging from 0^o to 60^o were analysed.

C_2 and CH monochromic projections are tomographically reconstructed to obtain their three-dimensional distribution, which allows the spatial correlation of C_2 and CH fields. The calculated evolution of maximum value of the mole fraction for C_2 and CH radicals shows that the maximum value of mole fraction occurs simultaneously for both radicals. Moreover, C_2 and CH radicals peak concentration increase until $\Phi = 1,4$, decreasing as the equivalence ratio increases up to $\Phi = 2$. C_2/CH ratio shows that the relative growth of C_2 is larger than CH, from $\Phi = 0.6$ to $\Phi = 1.4$. Above $\Phi = 1.4$, C_2 concentration decreasing is more intense than CH. Then, for well-mixed conditions of lean combustion, a low value of C_2/CH ratio is expected.

Detailed images of C_2 and CH spatial distribution produced within the combustion chamber are acquired to the fuel/equivalence ratio/vanes angle combinations analysed. The influence of swirl on the length and position of the propane premixed flame depicts that non-swirling flame stabilises using the bluff-body disk, spreading over a long section of the combustion chamber. As the swirl increases, a new recirculation zone is induced, bending the flame and concentrating the reaction zone within the first section of the combustion chamber. The maximum intensity value at both wavelengths is not altered due to the vanes angle. At $\Phi = 1$, CH intensity signal is stronger than C_2 within the range of vanes angle analysed.

CH dominates C_2 emission from $\Phi = 0.6$ to 1.2, but it was not detected any influence of the equivalence ratio on the flame shape. However, it was highlighted that small differences between the shape of CH and C_2 images can be explained due to the emission relaxation time of each free radical, namely 10^{-5} s for CH and 10^{-7} s for C_2, which allows that CH remain emitting while is transported to the recirculation zone, therefore presenting higher emitting areas than C_2.

The relationship between C_2/CH intensity ratio and equivalence ratio for propane burning shows that intensity ratio increases as equivalence ratio increases and that variation of intensity ratio at a given equivalence ratio is relatively small. For increasing equivalence ratio, the difference between the maximum and minimum values of C_2/CH ratio increases, probably caused by incomplete mixing.

Aeronautical liquid fuel flames analysis encompassed measurements performed at two fuel mass flow rate, namely Φ=0.5 and 0.8, and four vanes angle conditions, $\omega = 0$, 20, 35 and 55^o. In the non-rotational flow the smaller path length did not allow complete fuel vaporisation and air/fuel mixing processes, which was identified by the non-vaporised fuel droplets impinging the quartz wall and burning within the combustion chamber. Subsequent increasing of the swirling first centrifuges and concentrates the flame into the recirculation zone, following the same pattern presented by propane flows.

The present results provide new information on the characterisation of mixture homogeneity of lean premixing flames within practical combustion chamber geometry. The utilisation of local C_2/CH intensity ratio is related to equivalence ratio and can assess useful information on the quality of the mixing process, which can be used to improve the design of practical combustors. The results suggest that there is a qualitative compromise between light intensity and mixing conditions. However, it is necessary to stress this relationship between chemical species emission and mixing parameters in order to allow the quantification of the local equivalence ratio, and therefore the mixing process efficiency.

5 REFERENCES

Anacleto , P. and Heitor, M.V., 1997, Câmaras de Combustão com baixa Produção de Poluentes para Turbinas a Gás, Ingenium, 15, pp. 66-70.

Anacleto, P., 1993, Análise Experimental de uma Câmara de Combustão Axissimétrica com Pré-vaporização e Pré-mistura de Reagentes, Dissertação de Mestrado, Instituto Superior Técnico.

Bahr, D., 1995, Aircraft turbine engine NOx emission abatement, In: Unsteady Combustion, eds. F. Culick, M.V. Heitor and J. Whitelaw, Kluwer Academic Publ., NATO ASI Series, Vol. E306, pp. 243-264.

Chou, T. and Patterson, D.J., 1995, In-Cylinder Measurement of Mixture Maldistribution in a L-Head Engine, Combustion and Flame, 101(1/2), pp. 45-57.

Correia, D.P., Caldeira-Pires, A. , Ferrão, P., Heitor, M.V., 1998, 3D Flame Temperature Measurements Using a Combined Tomography/Radiation-Extinction-Model Technique, Combustion and Flame, submitted.

Costa, F.S., Caldeira-Pires, A., Anacleto, P., Carvalho-Jr., J.A., 1998, Flame Analysis through tomography: Caracterization of LPP Gas Turbine, ENCIT98, Rio de Janeiro - Brazil, December 3-7.

Fernandes, E., 1998, The Onset of Combustion-driven Acoustic Oscillations, Ph.D. Thesis, Instituto Superior Técnico, Dept. of Mechanical Eng., Lisbon, Portugal.

Gaydon, A.G., 1957, The Spectroscopy of Flames, Wiley, New York, p.159.

Joos, A. and Pelischeck, G., 1995, Low Emission Combustor Technology, In: Advances in Engine Technology, ed. Dunker, Willy & Sons Ltd, pp. 105-149.

Kee, R.J., Rupley, F.M., Miller, J.A., 1992, Chemkin-II: A Fortran Chemical Kinetics Package for the Analysis of Gas Phase Chemical Kinetics, Sandia National Laboratories Report SAND89-8009B, Reprinted.

Konnov, A.A., 1998, Detailed Reaction Mechanism For Small Hydrocarbons Combustion, Release 0.4, http://homepages.vub.ac.be/akonnov/.

Mokkadem, K., Perrin, M.Y., Rolon, J.C., Perrin, M. and Lewinsky, H.B., 1994, Flame Front Visualization by OH LIF and C2 Spontaneous Emission in Axisymmetric Laminar Methane-Air Premixed Flames, 7th Int. Symp. On Application of Laser Techniques to Fluid Mechanics, pp. 15.4.1-15.4.7.

Nguyen, Q-V. and Paul, P.H., 1996, The Time Evolution of a Vortex-flame Interaction observed via Planar Imaging of CH and OH, 26th Symp. (Int.) on Combustion, The Combustion Institute, pp. 357-364.

Yamazaki, M., Ohya, M. and Tsuchiya, K., 1990, Detection of the air equivalence ratio of a burner from the flame-emission spectra, Int. Chemical Engineering, 30, pp. 160-168.